

# Plan for Tagger Microscope Prototype Beam Test

I. Senderovich, R.T. Jones

October 18, 2010

## Abstract

The development of the high resolution tagger hodoscope for Hall D at Jefferson Lab has matured to the stage of prototype testing. A fully functional prototype with 5% of the required channels is ready for a beam test. This note presents a plan for the desired parasitic beam test downstream of the Hall B tagger, including the performance parameters under test, equipment requirements, space and time requested, and analysis methods.

## 1 Introduction

The University of Connecticut Nuclear Physics group, a member of the GlueX collaboration and its Tagged Beam Working Group is implementing a novel design for the tagging counters to be used in Hall D at Jefferson Lab. The design of the high resolution hodoscope referred to as the “tagger microscope” presents the challenge of very high electron flux of 20 MHz/cm on the spectrometer focal plane when the experiment operates at full design intensity. To maintain a reasonable tagging rate per channel, the tagging counters are set to be only 2 mm wide. They are composed of  $2 \times 2 \text{ mm}^2$  square scintillating fibers 2 cm long, aligned with their axis parallel to the electron trajectory. The fibers’ small cross-section matches the needs of tagger readout well: the 2 mm width gives an acceptable rate and a nearly perfect match to the intrinsic energy resolution of the tagging spectrometer [1]. Additionally, the 2 mm height of the fiber allows suppression of tags for electrons emitted with bremsstrahlung angles outside the forward direction. This brings tagger counter acceptance closer to that of the photon collimator, thereby improving tagging efficiency.

The focal plane is instrumented with a two-dimensional matrix of scintillation counters. During alignment, the entire array is read out and its alignment remotely adjusted such that the electron stripe across the focal plane is centered on a single row of fibers. Then, readout of all other rows, which count electrons in the tails of the vertical electron distribution shown in Fig. 1, is turned off. An additional benefit of this remote-control alignment scheme is the ability to switch between active tagging rows when radiation damage degrades the detection efficiency in a given row beyond tolerable levels.

Another novelty in the design of the Hall D tagger microscope is the use of silicon photo-multipliers (SiPMs) for readout. These new solid state photo-sensors have active areas that match the fiber cross sections well, are faster than photo-multipliers (PMTs) with roughly the same efficiency and gain, without the necessity of high voltage. Very importantly, they are insensitive to magnetic fields, and do not require magnetic shields to operate in the vicinity of the tagger dipole magnet. Use of SiPMs in the tagger microscope required the design of new preamplifier circuits and control electronics that incorporate robust real-time monitoring of bias voltages and temperatures in the readout.

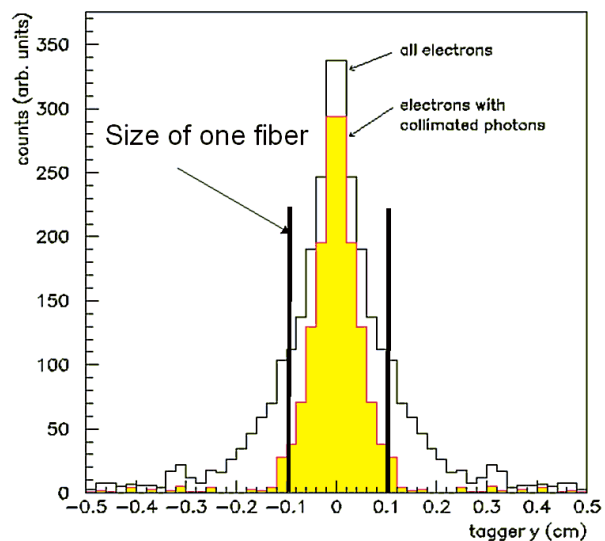


Figure 1: Simulated vertical distribution of the electrons on the focal plane. The open histogram shows the vertical impact position on the tagger focal plane of all electrons within the microscope energy range, whereas the solid histogram counts only those corresponding to photons that pass through the photon collimator. Suppressing the counting of electrons in the tagger whose photons will never reach the GlueX target has the effect of improving the tagging efficiency.

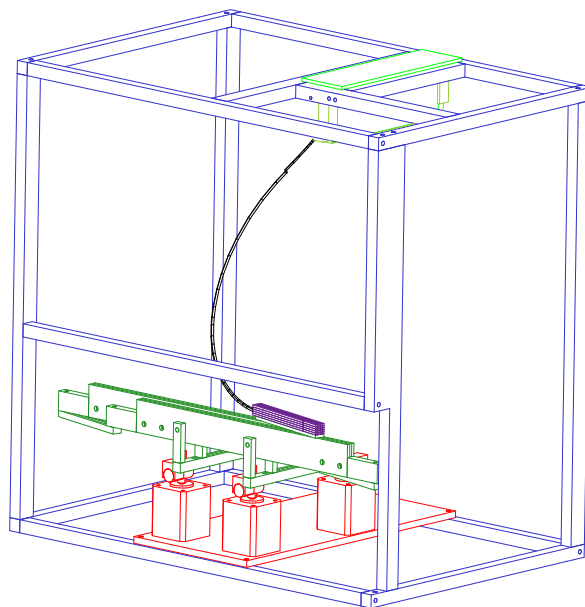


Figure 2: Rendering of the tagger microscope prototype chamber internals. Alignment mechanics, photo-sensor, and amplifier electronics, along with a single sample waveguide, are shown.

These systems have matured to the stage of testing under realistic beam conditions. A single module of fibers and associated electronics, 1 group out of the 20 comprising the full microscope, has been installed into a compact enclosure. Demonstrating that this prototype detector matches its specifications is best accomplished by placing it near the focal plane of an existing tagger and taking data parasitically during regular beamline operation. The Hall B tagger provides a unique opportunity to carry out these tests under conditions nearly identical to those to be found in Hall D. This constitutes an important validation of the tagger microscope design and construction plan, before the full detector assembly commences in 2012.

## 1.1 Design specifications

The following design specifications have been set forth for the tagger microscope:

1. time resolution of 200 ns rms
2. photons tagged with energy resolution better than 60 MeV within coherent peak
3. nominal operation at 100 MHz tagged photons in coherent peak after collimator
4. tagging rate 250 MHz within coherent peak at nominal intensity (about 2-4 MHz per channel)
5. average tagging efficiency at least 70% within coherent peak under nominal conditions

It has been determined from Monte Carlo studies that the technique for forward electron angle selection satisfies the tagging efficiency requirement and should be able to deliver the required tagged photon rate after the collimator. The ability to read out at the required rate seems to be within reach of the designed detector. This was shown by the initial studies as well as electronics-modeling calculations and bench testing. However, a beam test would be the most comprehensive exercise to confirm the adequacy of the current design with respect to the design specifications.

## 2 Detector Alignment

Fig. 3 shows the degree of signal sharing between adjacent scintillating fibers as a function of angle. When the fiber axis is aligned to within  $3^\circ$  of collinearity with the electron trajectory, a factor of 3 separation between adjacent signal amplitudes is seen. Certainly for a beam test, this is a very soft alignment criterion. The alignment features of the prototype described below demonstrated alignment to better than  $0.2^\circ$  on the bench.

Proper alignment to the electron crossing angle is configured to first order during fiber array assembly. Scintillating fiber support rails are set to force proper orientation. Additional corrections of  $\pm 3.5^\circ$  during installation in the Hall are possible using adjustment screws in the chassis of the prototype. All other angles and the selection of the exposed row in the two-dimensional fiber array are adjustable by step motors under remote control. The degrees of freedom available for online adjustment are shown in Fig. 4. While both aspects of alignment can be tested on the bench, the full exercise with a live beam will be very useful for checking the precision of the mechanical design and ease of online operation.

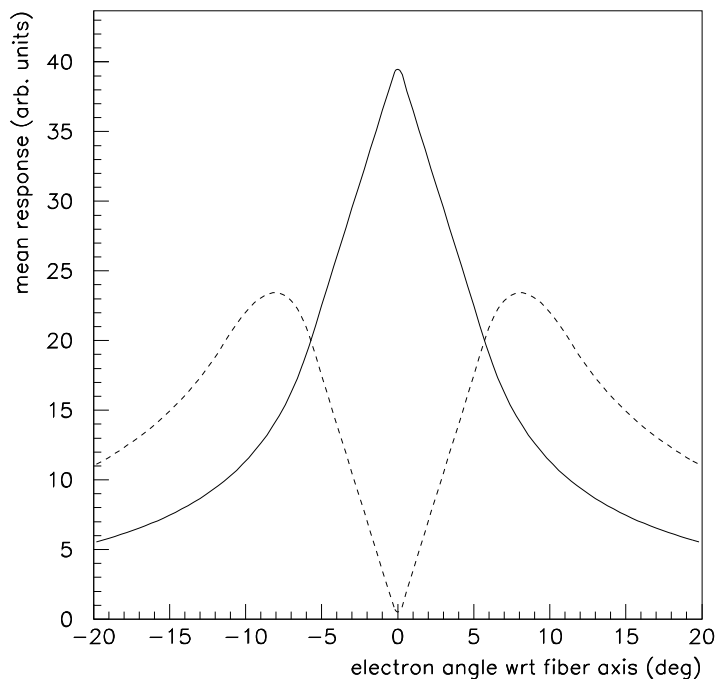


Figure 3: Response of a scintillating fiber (solid line) as a function of the angle between the electron track and the fiber axis is shown along with the response of the adjacent fiber (dashed line). The plot demonstrates good separation between signals in adjacent channels despite misalignment of several degrees.

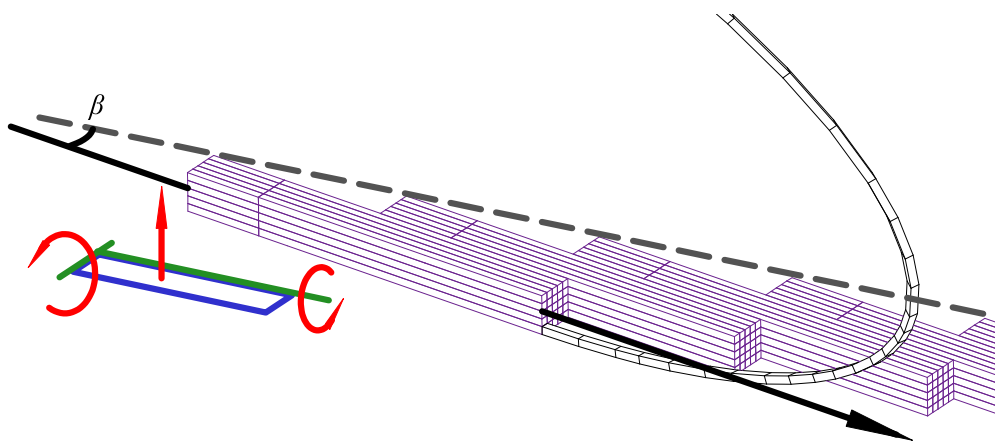


Figure 4: Visualization of the mechanical degrees of freedom of the scintillating fiber array. The actual scintillating fibers are the short segments in front of the longer clear waveguide fibers (all but one cut away in this schematic.) The angle  $\beta$  with respect to the focal plane is locked at the time of assembly.

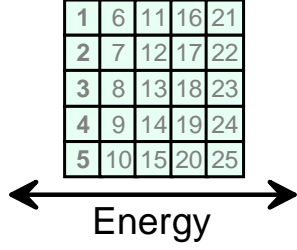


Figure 5: Scintillating fiber to SiPM mapping. The signal patch-through on the amplifier board is designed such that the the channels from the first column can be read individually. Otherwise signals are summed column-wise. The prototype readout is instrumented only for channels 1-19.

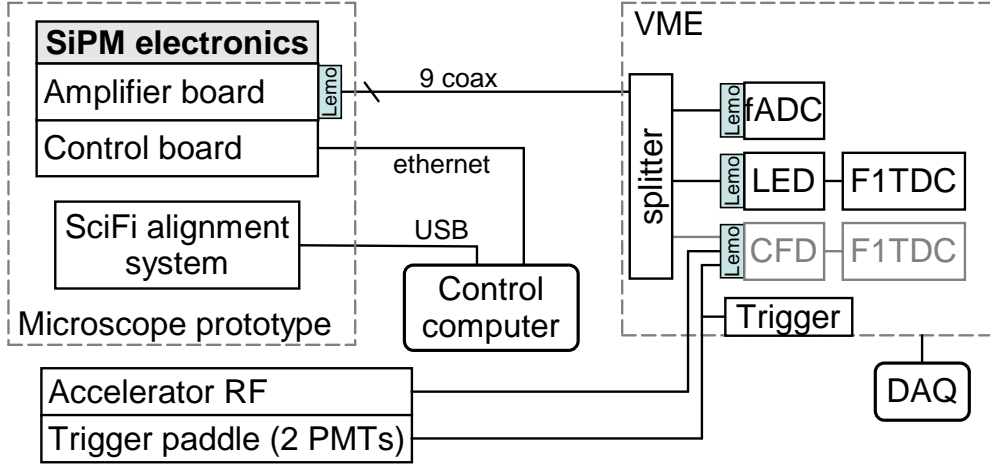


Figure 6: The scheme is shown for readout and control of the tagger microscope prototype during beam test. The CFD/TDC readout chain shown represents the requested instrumentation of some channels with these modules to serve as a reference for signal timing.

### 3 Readout

The proposed beam test will be the first time the SiPM signals from microscope prototype electronics are read out with the designated GlueX fADC and F1TDC modules. Examining the output on the equipment actually intended for reading out this detector component is essential at this point of development. The  $5 \times 5$  scintillator bundle is instrumented with SiPMs on 4 of its columns results in 9 channels of readout: 4 columns (where the individual channels are summed) and the 5 individual scintillators in the first column. The scintillating fiber matrix and its mapping to the SiPM channels is shown in Fig. 5. A diagram of beam test control and readout is shown in Fig. 6. As will be discussed in the following sections, the readout technique under test involves leading edge discrimination with time-walk correction using the pulse integrals taken from the fADC record.

#### 3.1 Time Resolution

One critical requirement for the microscope is the 200 ps time resolution. The random nature of atomic transitions in the scintillating fibers gives rise to a spread in time for the arrival of any given photon to the photo-detector. Bicon's (Saint-Gobain) BCF-20 scintillators have a decay time of 2.7 ns. Given that the collective photon emission time uncertainly goes as  $2.7 \text{ ns} / \sqrt{N_\gamma}$  a minimum of 183 detected photons is required to meet the 200 ps time resolution specification. The smeared signal from the scintillator is shown in Fig. 7. Simulations predict that the mean photoelectron

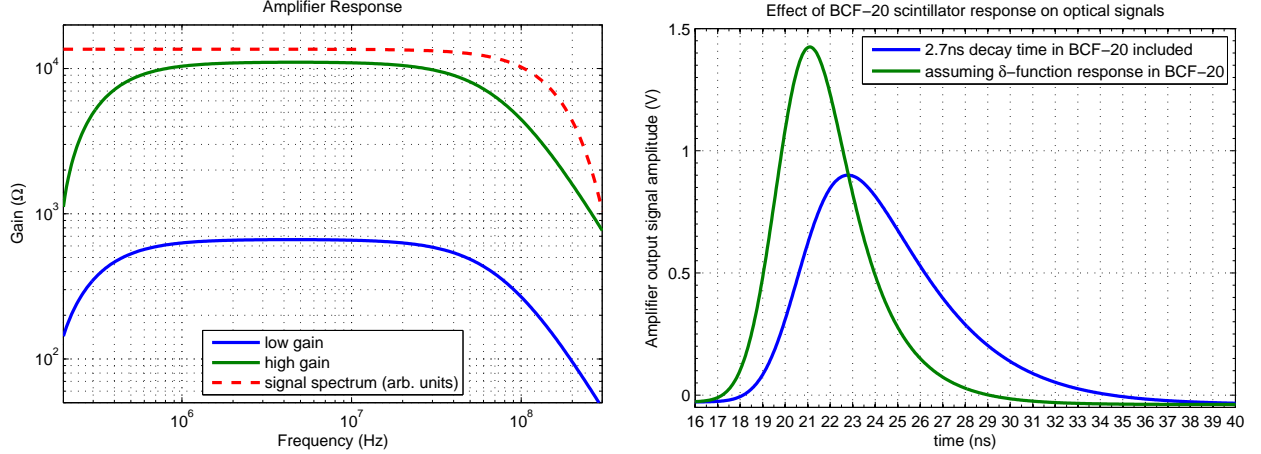


Figure 7: The left plot shows the calculated bandwidth of the microscope amplifiers plotted together with the spectrum of the bare SiPM signal. The plot on the right shows the expected shape of the signals coming from the tagger microscope (i.e. amplifier-filtered SiPM signal convolved with the scintillator response.)

count for the central fiber will be greater than 300, assuming that glue joint transmission factors and fiber-SiPM alignments are all within nominal specifications. This beam test provides the first real check of this prediction.

Adherence to the time resolution requirement will be checked both by looking at the photon statistics of scintillations in the beam and direct observation of the signal's walk in time. The first approach relies on the former calibration of the SiPM/amplifier gains conducted on the bench using photon counting techniques at low light levels. Knowing the gain, the average detected photo-electron yield can be determined. The more definitive latter approach takes an absolute time reference: the accelerator bunch timing signal (accelerator RF) and compares to the time determined by the TDC. An additional reference and a source of a trigger signal will be provided by the scintillator paddle mounted upstream of the prototype microscope counters (w.r.t. electron's trajectory.) This scintillator will be instrumented with PMTs on both sides for optimum time resolution and singles rejection.

In principle, there are two contributions to the time resolution that need to be disentangled. The first comes from the uncertainty involved in the photon statistics discussed above. The second contribution is from the walk due to leading edge discrimination. Abatement of this effect using pulse height correction using pulse integrals from the fADC needs to be tested. Indeed the efficacy of this correction must be examined closely because the relatively sparse 250 MHz sampling of the SiPM signals results in only about 4 samples per pulse, leading to uncertainty in the integral of the pulse. Separating these contributions to time resolution will require the use of constant fraction discriminators (CFD). We propose instrumenting up to four channels with CFD-F1TDC readout chains for time resolution comparison.

### 3.2 Efficiency

Another important performance parameter for the microscope is its tagging efficiency. Random arrival of tagging electrons in a single channel with finite pulse duration results in occasional

overlap of pulses such that the two leading edges can no longer be resolved. While calculation of the frequency of this effect using the measured pulse shape is effective and straightforward, measurement of the pulse selection efficiency in a real pipeline fed by pulses from an electron beam will be extremely useful.

### 3.3 Cross-talk

The degree of cross-talk between channels of the microscope is another matter that must be investigated in a live beam. Great care was taken to isolate the channels along their optical and electronic segments. It will be important to measure the degree to which these measures were successful. Also, it is understood that multiple scattering of electrons will still result in signal sharing among adjacent scintillating fibers.

Aside from measuring the total cross-talk fraction, it will be possible to separate the signal-sharing contribution near and in the photo-sensor electronics from other effects. Since signals from the  $5 \times 5$  scintillator grid are serialized on the amplifier board into a row of SiPMs (shown in Fig. 5,) certain pairs of adjacent amplifiers (e.g. 8 and 9 in Fig. 5) will correspond to neighboring scintillators from one column while other pairs (e.g. 10 and 11 in Fig. 5) will correspond to fibers across a column break. The fibers corresponding to the latter case is thought to be immune from signal sharing at their upstream end by virtue of their separation. Thus, such channel pairs will be measuring electronic cross-talk on the amplifier board and perhaps the optical cross-talk between adjacent fiber-SiPM junctions. Any excess signal sharing measured between channels with adjacent scintillators is interpreted as cross-talk at the upstream end: electron multiple scattering or optical cross-talk in case of a breach in the opaque fiber coating.

## 4 Beam Test Requirements

### 4.1 Space

The physical dimensions of the microscope prototype are about  $33 \text{ cm} \times 46 \text{ cm} \times 55 \text{ cm}$ . Fig. 8 shows the space in Hall B identified as perfectly suitable for testing the detector. It is currently an unoccupied space beneath the Hall B tagger cage, downstream of the spectrally analyzed electrons. A VME crate and a control computer may take any convenient location along the side of the cage.

### 4.2 Time Schedule

The current running of the PrimeX experiment in Hall B presents the ideal opportunity for this test. High beam current in the following TPE experiment with installation starting November 11, 2010 excludes this time from possible parasitic tests. Thus, time from now until November 11th is requested for the described tests.

### 4.3 Equipment

Given the performance characteristics that require beam testing described above, the following equipment is seen as necessary:

- (1) VME64x Flash ADC Module (12 bit fADC250)
- (1) LED board

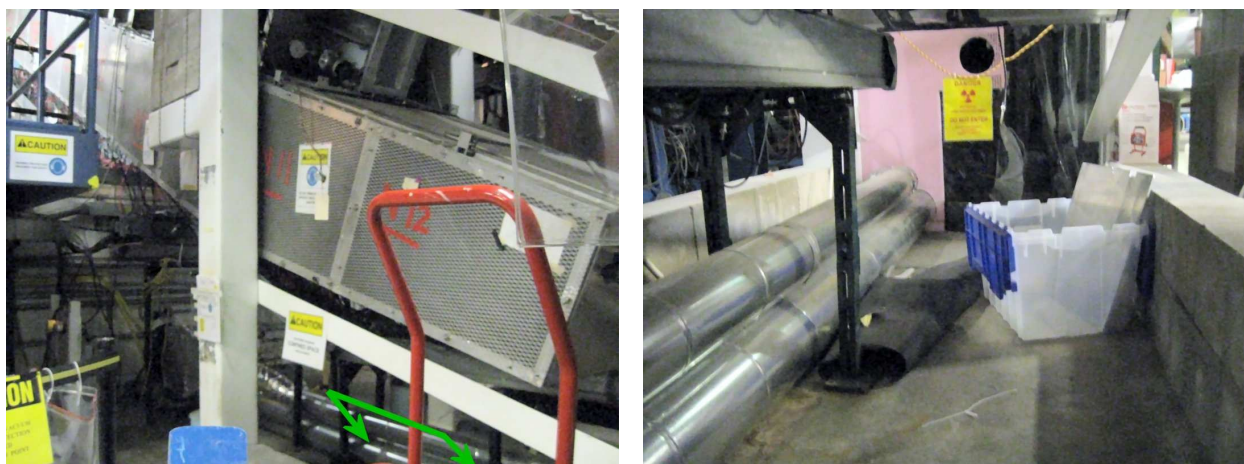


Figure 8: Space downstream of the Hall B tagger identified as suitable for testing the prototype of Hall D's tagger microscope. The bracket shown in the left photograph identifies the approximate position for the prototype's chamber. The photo on the right shows the empty space underneath the Hall B tagger cage.

- (1) F1TDC
- (1) CFD module is possible
- VME crate with a readout controller and trigger coordinator.
- Appropriate cables, splitters etc.
- Scintillator paddle with two (2) PMTs

All items in this list have been allocated aside from the last item: as of the writing of this document, assembly of the paddle is in progress. The required power supplies and control systems for the prototype tagger microscope itself will be provided by the Connecticut group.

## 5 Conclusion

The tagger microscope prototype for Hall D is fully ready for beam testing. All necessary bench tests have been carried out and equipment procured for this exercise. At this stage of development, the prototype will greatly benefit from the realistic test described in this document. Hall B during the next few weeks is the ideal place to carry this out.

## References

- [1] A. Somov, "Resolution studies of a dipole tagger magnet: response to the magnet review referees" GlueX-doc-1368 (2009).